CHEMCOMM
Feature Article
www.rsc.org/chemcomm

Nanoparticles as structural and functional units in surface-confined architectures

Andrew N. Shipway and Itamar Willner*

Institute of Chemistry, The Hebrew University of Jerusalem, Jerusalem 91904, Israel. E-mail: willnea@vms.huji.ac.il

Received (in Cambridge, UK) 12th June 2001, Accepted 22nd August 2001
First published as an Advance Article on the web 1st October 2001

The nanoscale engineering of functional chemical assemblies has attracted recent research effort to provide dense information storage, miniaturized sensors, efficient energy conversion, light-harvesting, and mechanical motion. Functional nanoparticles exhibiting unique photonic, electronic and catalytic properties provide invaluable building blocks for such nanoengineered architectures. Metal nanoparticle arrays crosslinked by molecular receptor units on electrodes act as selective sensing interfaces with controlled porosity and tunable sensitivity. Photosensitizer/electron-acceptor bridged arrays of Au-nanoparticles on conductive supports act as photoelectrochemically active electrodes. Semiconductor nanoparticle composites on surfaces act as efficient light collecting systems, and nanoengineered semiconductor 'core–shell' nanocrystal assemblies reveal enhanced photoelectrochemical performance due to effective charge separation. Layered metal and semiconductor nanoparticle arrays crosslinked by nucleic acids find applications in the optical, electronic and photoelectrochemical detection of DNA. Metal and semiconductor nanoparticles assembled on DNA templates may be used to generate complex electronic circuitry. Nanoparticles incorporated in hydrogel matrices yield new composite materials with novel magnetic, optical and electronic properties.

Introduction

Increasing interest is directed to miniaturization and the nanoscale engineering of functional chemical assemblies.[1] The development of nanoscale devices will provide dense information storage, ultra-small sensing units, and data processing elements of reduced dimensions. Another important aspect of miniaturization to the nanoscale is the breakdown of macroscopic properties and the emergence of quantum-level phenomena.[2] Metal and semiconductor nanoparticles exhibit unique properties and provide important building blocks for the construction of functional structures.[3] Nanoparticles can be synthesized from a variety of materials with controllable sizes, shapes and morphologies.[4] The electronic properties of nanoparticles, which may be tuned by the particle dimensions, give rise to unique absorbance and emission features.[5] The confined electrons in nanoparticles smaller than the wavelength of light give rise to plasmon excitons.[6] Nanoparticles also offer catalytic properties that differ from the bulk material properties, due to their high surface-area, high edge concentration and unusual electronic properties.[7] This has led to the application of modified nanoparticles in enantioselective catalysis[8] and electrocatalysis on surfaces.[9]

The surface modification of nanoparticles by functional monolayers or polymer 'shells', provides a means to generate composite materials with tunable surface properties (*e.g.* wettability, hydrophobicity, polymerizable units, photosensitive sites or molecular recognition properties).[10] In addition, the surface functionalization of nanoparticles allows their covalent attachment, self-assembly and organization on surfaces.[11] The engineering of nanoparticle surfaces has led to the construction of nanoparticle dimers and trimers,[12,13] controlled aggregates,[14,15] wires[16] ordered monolayers[17] and multilayers.[18] The integration of functional nanoparticles with surfaces has enabled the organization of nanoscale devices[19] including single-electron devices.[20] In this account we focus on the use of modified nanoparticles as structural or functional units in the assembly of composite structures on surfaces. We address the use of the nanoengineered architectures as high surface-area conductive matrices, as optical indicators, and as semiconductor composites for photoelectrochemical functions. We discuss the use of surface-confined architectures for sensoric and photoelectrochemical applications and focus on the tailoring of composite materials with novel electronic properties. We also introduce the conjugation of nucleic acids with nanoparticles for the development of DNA sensors and complex electronic circuits.

Nanoparticle multilayers in sensing applications

The use of metal nanoparticles as conductive elements in electrochemical sensing interfaces has been approached in several different ways. One direction involves the use of gold nanoparticles to contact biocatalysts either by the fabrication of nanoparticle–enzyme conjugates[21] or by the sequential immobilization of the nanoparticles and the biomaterial.[22] The small size of the nanoparticles not only gives a conductive matrix, but also enables them to approach the redox sites of some enzymes closely enough to provide electrical communication between the enzyme redox-center and the electrode, without the need for a diffusional electron mediator. The conductivity of metal nanoparticles also allows their use as gas sensors. Thin films of gold nanoparticles held apart by long chain thiols demonstrate a conductivity that is strongly dependant on gas vapors.[23] The vapors are absorbed by the nanoparticle–thiol matrix, modulating the conductivity of the film (as is also the case in carbon black–polymer composites[24]).

A series of sensors has been developed using Au-nanoparticle multilayers crosslinked by molecular host components. Scheme 1 outlines the general method for the construction of the multilayer Au-nanoparticle structures. First, a conductive glass support is functionalized with a thin film of 3-(aminopropyl)siloxane to yield a positively charged interface. The electrostatic binding of the negatively charged citrate-stabilized Au-nanoparticles (12 ± 1 nm diameter) yields the first layer of Au-nanoparticles.[25] Treatment of the negatively charged interface with the tetracationic cyclophanes cyclobis(paraquat-*p*-phenylene) **1**[26] or cyclobis(paraquat-*p*-biphenylene) **2**,[27] the bipyridinium salts **3** or **4**, or the octacationic Pd(II)-macrocycle **5**,[28] results in the electrostatic association of the molecular host

components. Further interaction of the assembly with the citrate-capped Au-nanoparticles yields the second layer of nanoparticles, and by the alternating treatment of the system with the oligocationic molecular crosslinker and the nanoparticles, an architecture of the desired thickness may be constructed. The crosslinking units need not necessarily be molecules. Analogous results have been obtained using charged polymers,[29] other nanoparticles[30] and even biomaterials.[31] Similarly, covalently linked multilayers can be constructed using gold-binding bisthiol molecules as crosslinkers.[32]

Fig. 1 shows the characterization of 1–5 layers of gold nanoparticles crosslinked by the tetracationic cyclophane cyclobis(paraquat-*p*-phenylene) **1**. The absorbance spectra [Fig. 1(A)] show the characteristic plasmon absorbance of the gold nanoparticles at *ca*. 520 nm,[33] and as more layers are added, an additional absorbance appears at longer wavelengths as a

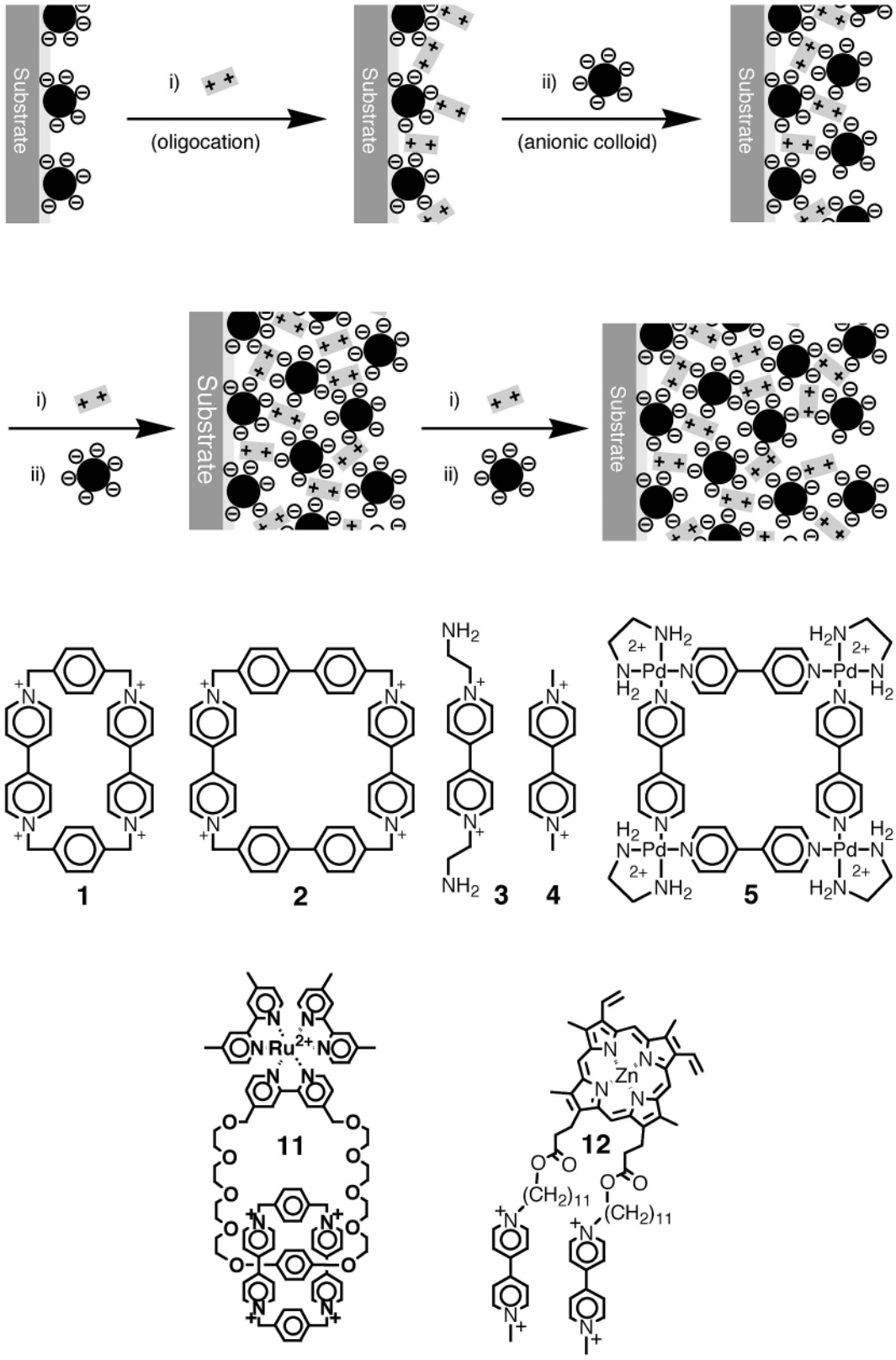

Scheme 1 Method for the construction of oligocation-crosslinked Au-nanoparticle multilayers by electrostatic interactions. The first nanoparticle layer is formed by the interaction of a nanoparticle solution with an amine-functionalized surface.

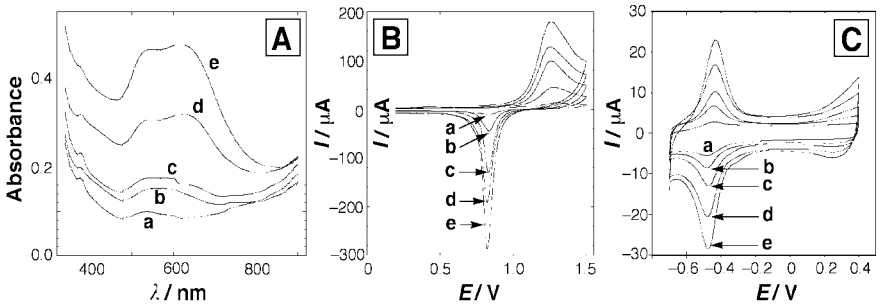

Fig. 1 (A) Absorbance spectra of a glass slide after (a–e) the deposition of 1–5 **1**-crosslinked Au-nanoparticle treatments. (B) Cyclic voltammograms of the Au-surface of **1**-crosslinked assemblies containing (a–e) 1–5 layers of Au-nanoparticles. (C) Cyclic voltammograms of **1** in (a–e) 1–5 layer arrays of **1**-crosslinked Au-nanoparticles.

consequence of interparticle plasmon coupling.[34] Electrochemical analysis of the gold surface [Fig. 1(B)] and the cyclophane crosslinking units [Fig. 1(C)] demonstrate the almost linear buildup of the structure on the conductive support. The fact that the nanoparticles and crosslinker continue to be electrochemically active throughout the crosslinked structure, demonstrates that the array is both porous and conductive. Coulometric assay of the electrical responses of the Au-nanoparticles and the bipyridinium units, indicates that the average surface coverage of the Au-nanoparticles per layer is *ca.* 1×10^{13} particles cm^{-2} and that *ca.* 100 units of **1** are associated with each Au-nanoparticle in the 3D structure.

The crosslinker **1** acts as a π-acceptor and is capable of forming π donor–acceptor complexes.[35] Thus, the association of electroactive π-donor substrates to the π-acceptor receptor sites, together with the 3D conductivity of the nanoparticle architecture, enables electrochemical sensing of the substrates. The cavity of **1** is suited to bind *p*-hydroquinone **6** and other hydroquinone derivatives such as dihydroxyphenylacetic acid **7**, dopamine **8** and adrenaline **9**. All of these substrates can be electrochemically sensed by the **1**-crosslinked Au-nanoparticle architectures assembled on the conductive glass supports.[36] The sensitivity of the functionalized electrodes is controlled by the number of nanoparticle layers in the structures.

Fig. 2(A) shows the electrochemical analysis of *p*-hydroquinone **6** by a 5-layer **1**-crosslinked Au-nanoparticle-functionalized electrode. The sensitivity limit for the sensing of **6** was estimated to be 1 μM. The substrate could not be electrochemically detected in this concentration range by a 5-layer Au-nanoparticle architecture crosslinked by the dicationic *N,N′*-dimethyl-4,4′-bipyridinium unit **3**. These results clearly indicate that the electrochemical sensing of **6** does not originate from the increase in the surface roughness of the electrode, but rather from the concentration of **6** in the receptor sites by supramolecular interactions. Fig. 2(B) exemplifies the electrochemical detection of adrenaline **9** by the **1**-crosslinked Au-nanoparticle array. The electrochemical oxidation of **9** associated with the receptor-sites reveals a broad irreversible wave that leads to a cyclic product that exhibits a reversible-redox response (wave x). The latter wave may act as an indicator for the concentration of adrenaline in the system [Fig. 2(B) inset].

The specificity of sensing by the Au-nanoparticle array is controlled by changing the structure of the crosslinking receptor units.[37] A three-dimensional array of Au-nanoparticles was constructed using the enlarged cyclophane, cyclobis(paraquat-*p*-biphenylene) **2**, Scheme 1. This larger receptor accommodates bishydroxymethylferrocene **10** as a guest. Fig. 3(A) shows the analysis of **10** (1×10^{-6} M) by the **2**-crosslinked Au-nanoparticle electrodes with different numbers of crosslinked Au-nanoparticle layers. As the number of layers increases, the electrical response of **10** is enhanced, demonstrating tunable sensitivity of the nanostructured layered electrode. Fig. 3(B) shows the amperometric responses of the Au-nanoparticle array upon the sensing of different concentrations of **10**. The resulting receptor-crosslinked arrays also reveal selectivity. While **10** is electrochemically sensed by a **2**-crosslinked Au-nanoparticle structure, the receptor **2** is too large to accommodate *p*-hydroquinone **6** in its cavity. Similarly, the **1**-crosslinked Au-nanoparticle assembly is unable to accommodate **10**, but does associate with *p*-hydroquinone, which is electrochemically sensed [Fig. 3(C)]. Selectivity is also observed upon the sensing of *p*-hydroquinone **6** by the Pd(II)-square, **5**-crosslinked Au-nanoparticle structure that is unable to detect the isomer *o*-hydroquinone. The selective sensing of **6** by the oligocationic

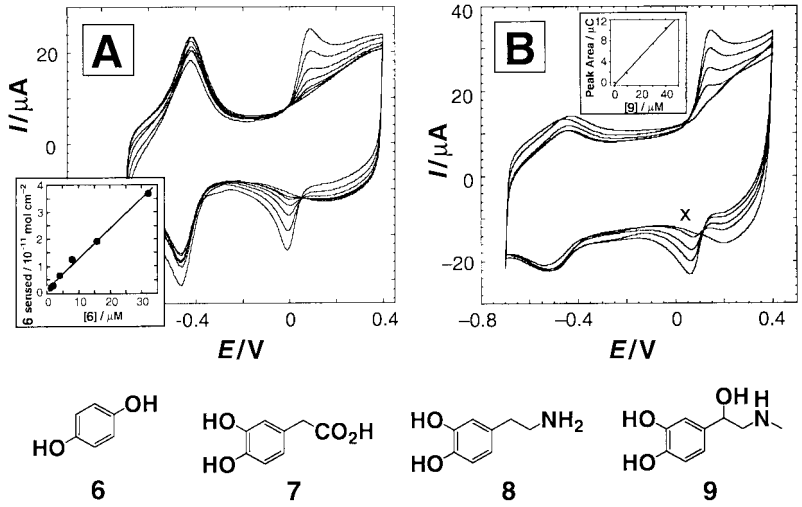

Fig. 2 (A) Cyclic voltammograms for the sensing of hydroquinone **6** (1–30 μM) by a 5-layer **1**-crosslinked Au-nanoparticle array. Inset: calibration curve for the sensing of **6**. (B) The sensing of adrenaline **9** (1–40 μM) by the array. [Wave (x) corresponds to the redox response of an electrocyclized product originating from the oxidized **9**] Inset: calibration curve for the sensing of **9**.

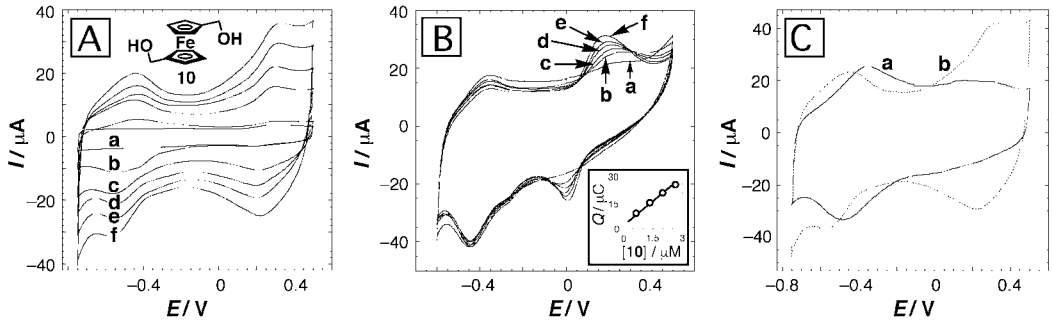

Fig. 3 (A) Cyclic voltammograms for the sensing of **10** (1 μM) with (a–f) 0–5 layers of **2**-crosslinked Au-nanoparticles. (B) The sensing of **10** (a–f = 0.1, 0.2, 0.4, 0.8, 1.5 and 3.0 μM, respectively) by a 5-layer **2**-crosslinked Au-nanoparticle array. (C) Cyclic voltammograms of 5-layer electrodes constructed using cyclophanes **1** (curve a) and **2** (curve b) as crosslinkers in the presence of **10** (1 μM).

macrocycle was attributed to the diagonal association of **6** to the Pd(II)-receptor, that is not possible for the *ortho* isomer.[38]

Receptor-modified Au-nanoparticles were also assembled on the gate interface of an ion-sensitive field-effect-transistor (ISFET).[39] A **1**-functionalized Au-nanoparticle ISFET device was found to effectively detect adrenaline, serotonin and dopamine. Since the ISFET gate-potential is controlled by the charge associated with the interface, the detection of receptor-bound substrates is not limited to electroactive species.

Nanoparticle multilayers in photoelectrochemical applications

The high surface-area, porous and conductive properties of Au-nanoparticle arrays can be exploited for the construction of photoelectrochemically active superstructures. Fig. 4(A) and (B) show absorbance spectra and cyclic voltammograms of a

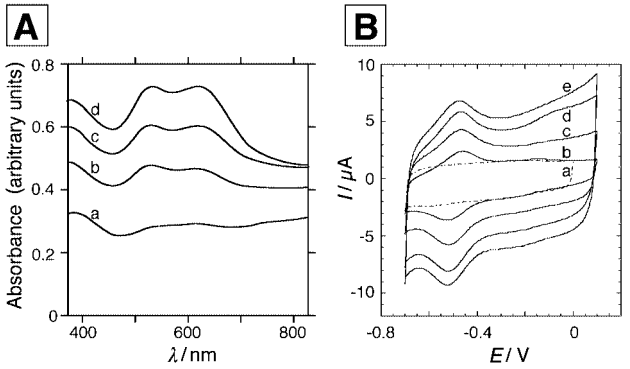

Fig. 4 (A) Absorbance spectra of (a–d) 1–4 layer Au-nanoparticle superstructures crosslinked by the catenane **11**. (B) Cyclic voltammograms of (a) a single nanoparticle layer, and (b–e) 1, 3, 4 and 5-layer **11**-crosslinked Au-nanoparticle arrays.

gold nanoparticle multilayer architecture 'crosslinked' by the hexacationic catenane **11**.[40] This catenane consists of non-covalently bound ruthenium tris(bipyridine) (photosensitizer) and bipyridinium (electron acceptor) groups.[41] The absorbance spectra show similar features to those of other molecule-crosslinked gold nanoparticle arrays, as well as an additional absorbance at 425 nm that is attributed to the ruthenium tris(bipyridinium) chromophore. Coulometric assay of the cyclic voltammograms corresponding to the bipyridinium crosslinking units reveals an almost linear increase in the surface coverage of the crosslinking units upon the build-up of the layers. The derived surface coverage of **11** per layer is 3.6×10^{-12} mol cm^{-2} and it has been estimated that on average *ca.* 45 units of the photosensitizer/acceptor crosslinker are associated with each Au-nanoparticle. Irradiation of the **11**-crosslinked Au-nanoparticle multilayer array results in the photocurrent action spectra shown in Fig. 5(A), which follows the absorbance features of the Ru(II)–tris(bipyridinium) chromophore. The photocurrent increases upon the build-up of the array and is reversibly cycled between 'ON' and 'OFF' states upon switching the light on and off, respectively. Fig. 5(B) shows the dependence of the photocurrent intensity on an applied potential. The photocurrent decreases as the potential is negatively shifted and it is blocked at a potential where the bipyridinium units are reduced to the radical cation. This observation led to the conclusion that the photocurrent originates from the primary electron transfer quenching of the excited Ru(II)–tris(bipyridine) chromophore by the bipyridinium electron acceptor. The reduced acceptor acts as an electron mediator for charge injection into the electrode, Fig. 5(C). Upon the electrochemical reduction of the bipyridinium units, intramolecular electron transfer quenching is inhibited and photocurrent generation is blocked. The nanoengineered electrode operated at a quantum efficiency of 1×10^{-4} in the generation of the photocurrent. A related nanoparticle engineered electrode for photocurrent generation using Zn(II)-protoporphyrin IX–bis(bipyridinium) photosensitizer–electron acceptor (**12**) as a crosslinker has also been developed.[42]

Photoelectrochemical electrodes based on semiconductor nanoparticles offer many advantages in the organization of

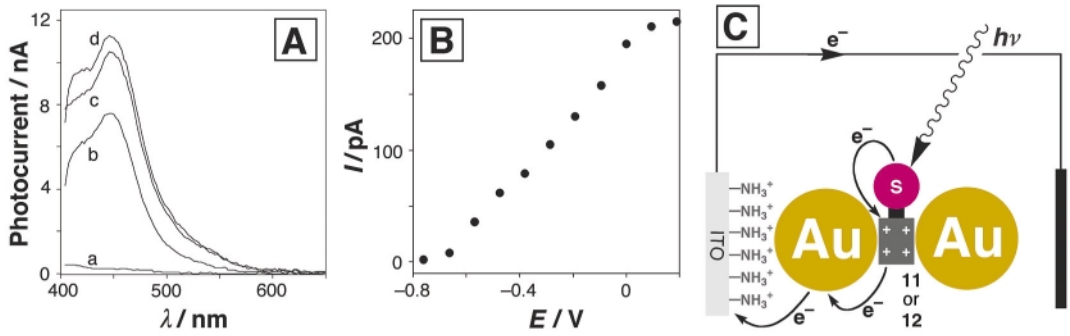

Fig. 5 (A) Photocurrent action spectra (a–d) obtained from 0-, 1-, 3- and 4-layer **11**-crosslinked Au-nanoparticle arrays. (B) Dependance of the photocurrent on the electrode potential. (C) Mechanism for the generation of a photocurrent from a photosensitizer(s)–bipyridinium dyad-crosslinked Au-nanoparticle superstructure.

energy conversion and storage cells. The ability to process, engineer and chemically functionalize semiconductor nanoparticles, enables the control of the properties and functions of the resulting photoelectrochemical cells. The use of nanoparticle-functionalized electrodes for photoelectrochemical applications has been reviewed in depth,[43] and the development and commercialization of solar cells based on photosensitizer/TiO_2 nanoparticle structures[44] represent recent advances in the field. Also, a large number of diverse nanoparticle-based electroluminescent devices have been investigated.[45] The tuning of the band-gap energies and redox properties of the energy levels by controlling the nanoparticle dimensions allows the tailoring of multicomponent systems that reveal new functionalities as a result of interparticle electronic coupling, and interparticle electron or energy transfer.[46] One example of such a system would be a nanoparticle-based 'luminescent collector'.[47] This is a device consisting of a thin sheet of material doped with dyes that absorb ambient light and re-emit it within the material where it is trapped by internal reflection. In order to collect a high proportion of the incident radiation, several chromophores with complementary absorption bands are required. Previous designs have led to problems of finding sets of organic dyes with this complementarity as well as the necessary processing and stability properties,[48] but nanoparticles may offer a feasible alternative.

Interparticle energy transfer between nanoparticles of the same substance but of different sizes exemplifies how multiparticle systems might find applications. It has been shown that both for indium phosphide[49] and cadmium selenide[50] nanoparticles, energy transfer from smaller to larger particles takes place within composite films. Fig. 6 shows absorbance and emission spectra of a 4 : 1 mixture of 2.8 and 3.7 nm-diameter CdSe nanoparticles that were prepared in highly monodisperse samples by selective precipitation. In a dilute solution (curve a), the emissions of both nanoparticles are seen, but in a close-packed film (curve b), energy transfer takes place and emission only from the larger particles is observed.

Extensive recent research effort has been directed towards the assembly of composite nanocrystalline semiconductor films to enhance the activity of photoelectrochemical cells. The coupling of a large bandgap semiconductor with a smaller bandgap semiconductor not only extends the photoresponse of the system to longer wavelengths but also facilitates charge separation. The photogenerated electrons and holes are trapped

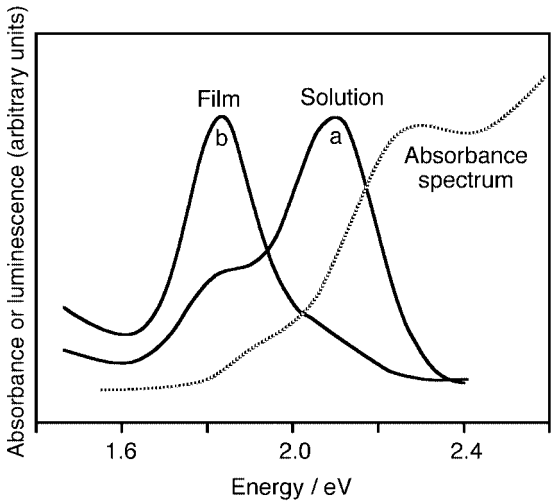

Fig. 6 Absorbance (----) and emission spectra of a 4 : 1 mixture of 2.8 nm and 3.7 nm InP 'quantum dots' (a) in solution, and (b) in a close-packed film.

into different particles, and the interparticle interface acts as a barrier for the recombination of the intermediate redox species. Fig. 7(A) shows the energetics of a SnO_2/CdSe nanocrystalline film assembled on an OTE electrode.[51] This photoelectrochemical electrode was found to operate at an efficiency of 2.25% ($I_{sc} \approx 30$ μA cm^{-2}; V_{oc} = 0.5–0.6 V; ff = 0.47), higher than for nanocrystalline CdS alone. The enhanced photoelectrochemical activity of the composite film is attributed to the charge rectification resulting from interparticle electron transfer. The role of coupled systems in enhancing charge separation has been demonstrated in other systems such as ZnO/CdS[52] and TiO_2/CdS.[53] Photosensitization of nanocrystalline composites results in charge rectification and facilitates the collection of the injected electrons by the electrode. Fig. 7(B) shows a 'core–shell' nanocomposite of TiO_2 coated with Nb_2O_5. Photoejection of electrons from an excited dye [*cis*-di(isothiocyanato)-*N*-bis(4,4′-dicarboxy-2,2-bipyridine)ruthenium(II)] to the Nb_2O_5 conduction-band followed by electron transfer to the TiO_2 conduction band results in the rectification effect. The recombination of the 'core' conduction-band electrons with the oxidized dye are retarded by means of the Nb_2O_5 'shell'.[54] This charge separation improves the photo-

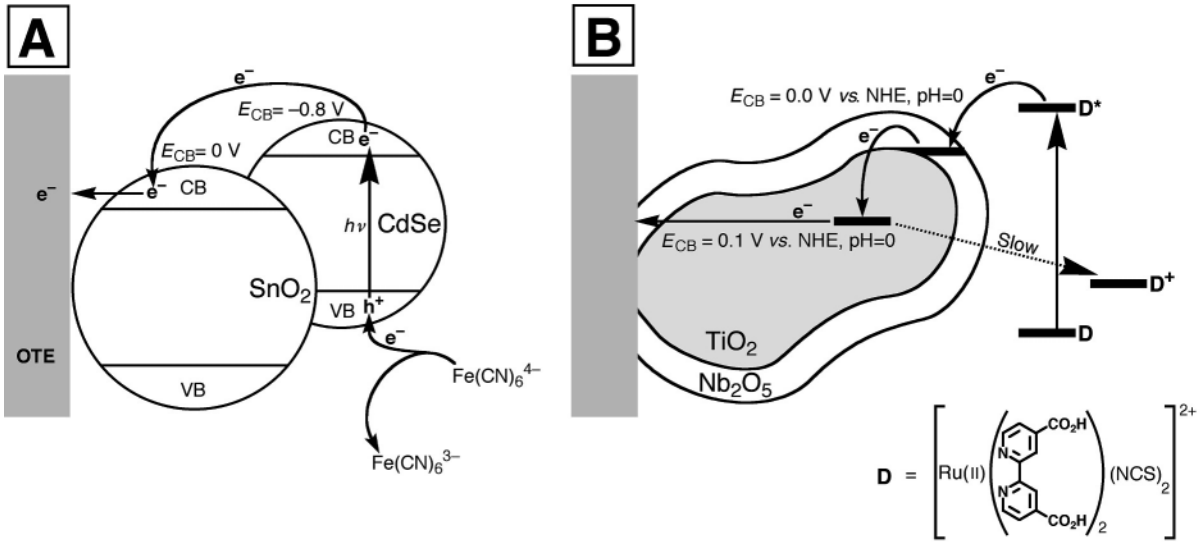

Fig. 7 (A) Suppression of charge recombination in a coupled SnO_2/CdSe system. (B) Charge separation upon photosensitization of a TiO_2/Nb_2O_5 core–shell semiconductor nanocomposite electrode.

electrochemical performance of the cell as compared to the TiO_2/dye system (maximum power of the TiO_2/Nb_2O_5/dye cell is 4.70 mW cm^{-2} as compared to 3.45 mW cm^{-2} for the TiO_2/dye cell). Similar results have been observed for other photosensitized nanocrystalline systems.[55]

DNA-linked nanoparticle superstructures

The study of DNA–nanoparticle conjugates has received special attention in the past few years. DNA is of particular interest since it may be made into complex, highly designed structures.[56] The use of DNA–nucleic acid-complementary binding, along with enzymes that act specifically on DNA (*e.g.* polymerase, ligase, endonuclease for polymerization, lengthening and scission, respectively) make it a useful structural tool. The dimensions and properties of DNA are well known and may be exploited, for instance for the fabrication of conductive wires.[57] In solution, interactions between DNA-functionalized-nanoparticles and DNA-crosslinked nucleic-acid-functionalized nanoparticles have been used for the detection of DNA,[58] and more recently they have allowed the construction of nanoparticle architectures on surfaces.[59] Scheme 2 shows a general method to fabricate a crosslinked multilayer of nanoparticle–DNA composites. First, an appropriate surface (gold or functionalized glass) is reacted with a thiolated oligonucleotide (**13**). This immobilized DNA can hybridize with part of an analyte nucleic acid (**14**) that is complementary with it. The remaining part of the analyte oligonucleotide can then be used to immobilize a nanoparticle that bears an oligonucleotide complementary to it (**15**). The growth may be continued either by reacting with the analyte then a nanoparticle functionalized by **13** [Scheme 2(A)], or by reacting with both at the same time [Scheme 2(B)]. This second layer contains many more nanoparticles since the first immobilized nanoparticles constitute 'branching points'. This 'amplification' allows the microgravimetric sensing of the analyte–DNA at concentrations of 1×10^{-10} M using a quartz-crystal-microbalance as transducer.[59a] If the analyte DNA has a sequence that is not properly complementary to both the surface and the nano-

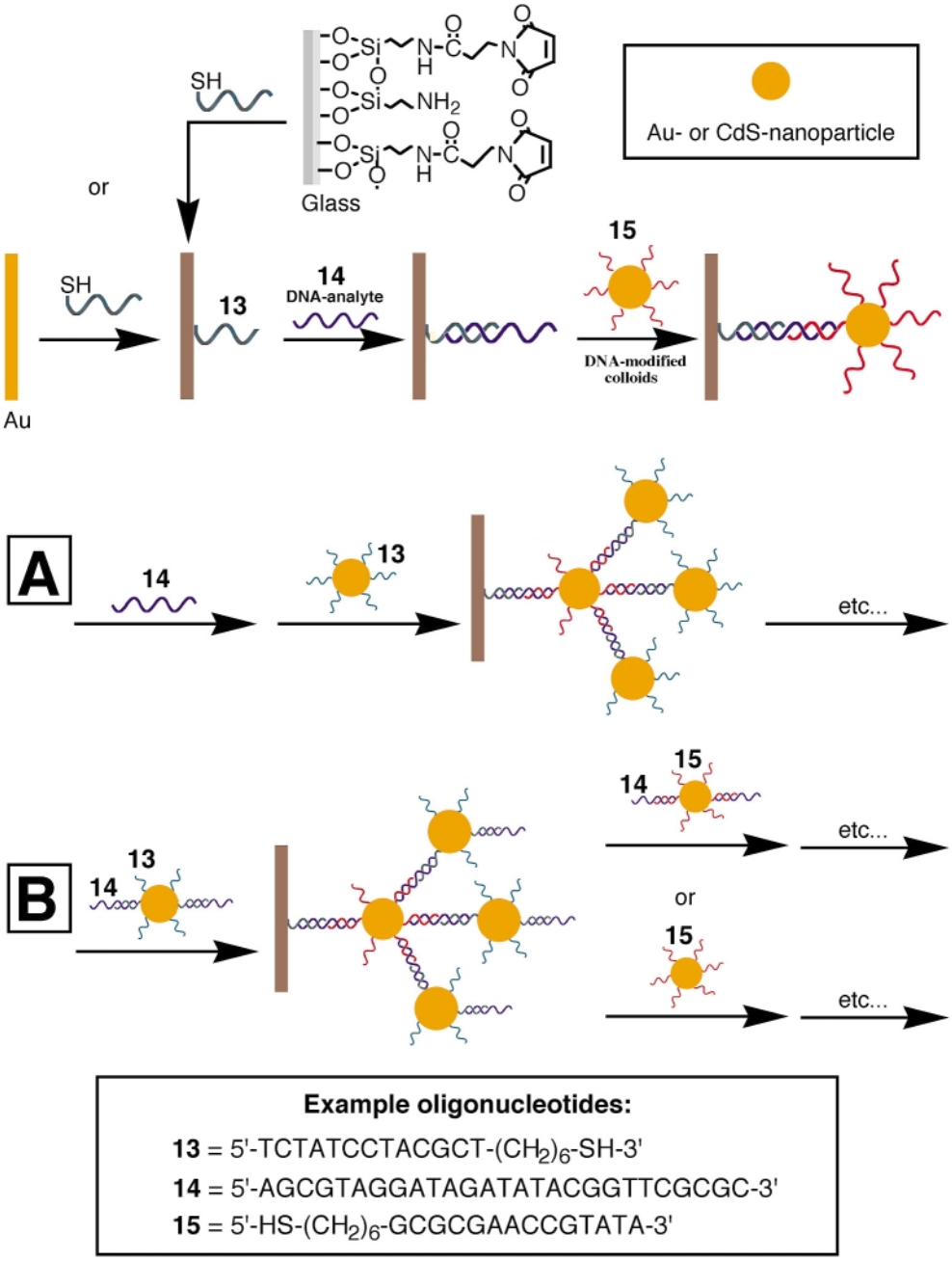

Scheme 2 Method for the construction of DNA-crosslinked metal or semiconductor nanoparticle arrays for the sensing of a DNA analyte, on gold or glass substrates. (A) Continued stepwise growth. (B) Growth with pre-hybridized nanoparticles and analyte.

particle, then the structure is not built up, and no response is measured. Fig. 8 shows results from a similar experiment, where several nanoparticle layers were constructed, and the concentration of the nucleic-acid functionalized nanoparticles and analyte DNA are sufficiently high to generate saturated Au-nanoparticle layers.[59b] Fig. 8(A) shows the absorbance spectra recorded for 1–5 nanoparticle layers. It is seen that non-linear growth only occurs for the first two layers, after which the surface is saturated with nanoparticles and a full layer is added at each step. It is also noteworthy that no additional absorbance above 600 nm appears, which indicates that the nanoparticles are not close enough to develop interparticle coupled plasmons. Finally, as the film becomes thicker, the melt transition for the DNA complex becomes sharper [Fig. 8(B)]. This observation is indicative of the cooperative effect of the nanoparticle network holding the entire assembly together.

Another way to transduce the build-up of these nanoparticle–DNA arrays is to employ functional nanoparticles. The use of cadmium sulfide nanoparticles (CdS) (instead of gold) yields a superstructure with novel fluorescence and photoelectrochemical properties.[60] Absorbance and fluorescence spectra of such a system are shown in Fig. 9(A). Irradiation of the array in the presence of a sacrificial electron donor results in a photocurrent that can also be used as a sensing signal [Fig. 9(B)]. The photocurrent is enhanced as the number of aggregated layers increases. It is also clear that the photocurrent increases non-linearly since the non-particle architecture exhibits a dendritic structure upon aggregation of the layers. Only CdS particles that are in intimate contact with the electrode support are active in the generation of the photocurrent. This was proved by the association of $Ru(NH_3)_6^{3+}$, acting as an electron acceptor, on the DNA strands. The $Ru(NH_3)_6^{3+}$ units trap the conduction-band electrons and mediate their transfer to the electrode, thus enhancing the generated photocurrent.

Hydrogel-entrapped nanoparticle systems

Polymers are extensively used as matrices for processing nanoparticles, and the advances in the assembly of polymer–nanoparticle composites have recently been reviewed.[61] As this review emphasizes the properties and functions of organized nanoparticle architectures, we will specifically discuss the functional features of nanoparticle–hydrogel composites. Hydrogels are highly swollen crosslinked polymers that are generally based on poly(acrylamide) and poly(acrylic acid). Due to the delicate balance of hydrogen bonds that stabilizes the gel's structure, the degree of swelling is highly dependent on factors such as solvent, solutes, pH, temperature and electric fields.[62]

'Ferrogels' are a class of materials that consist of magnetic nanoparticles (or 'ferrofluids') immobilized in hydrogel matrices. Poly(vinyl alcohol)[63] and poly(acrylamide)[64] hydrogels containing 10–12 nm magnetite (Fe_3O_4)[63] or maghemite (γ-Fe_2O_3)[64] particles have been investigated. These magnetic nanoparticles do not aggregate in solution as their mutual attraction is compensated for by repulsion due to surface charges and by loss of alignment of magnetic moments because of Brownian motion. The ferrogels can thus be prepared by a solution-state polymerization in the presence of the particles. Upon exposure to non-uniform magnetic fields, ferrogels deform almost instantaneously, and they return reversibly to their original state when the field is removed. Fig. 10 shows a typical experimental setup. The ferrogel is tethered to a stress-sensitive device from above, and a solenoid is placed below it.

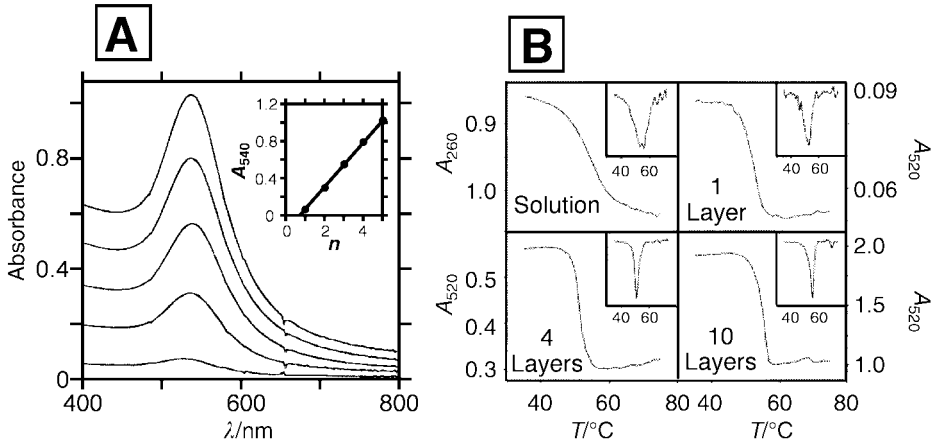

Fig. 8 (A) UV–VIS absorbance spectra of 1–5 Au-nanoparticle layers constructed on glass and linked by DNA (by method A, Scheme 2). Insert: growth of absorbance at 540 nm (A_{540}) with the number of layers (n). (B) Melt transitions of a DNA complex in solution, and the same complex as a nanoparticle linker in architectures of 1, 4 and 10 layers; monitored by absorbance at 260 nm (in solution) or at 520 nm (on surfaces). Insets: first derivatives of the melt curves.

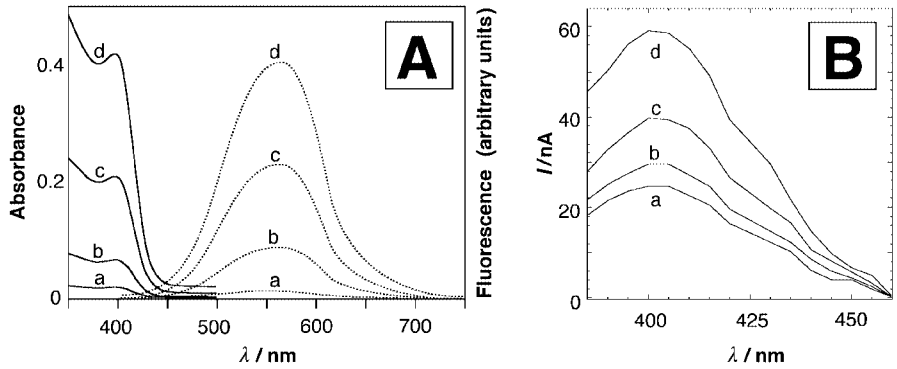

Fig. 9 (A) Absorbance (—) and fluorescence (·····) spectra of (a–d) 1–4 layer 'dendritic-type' DNA/CdS superstructures. (B) Photocurrent spectra of 2-layer (a and c) and 4-layer (b and d) DNA/CdS arrays in the absence (a and b) and presence (c and d) of $Ru(NH_3)_6^{3+}$.

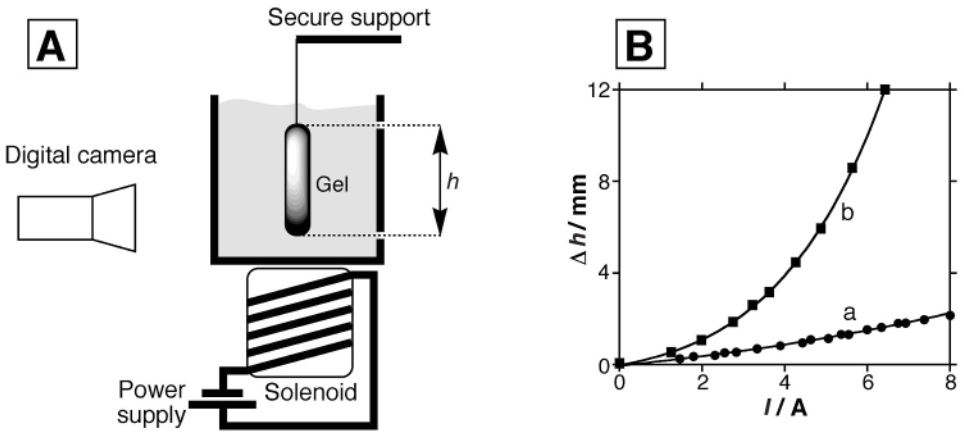

Fig. 10 (A) Experimental setup for the measurement of ferrogel elongation in a non-uniform magnetic field. (B) Elongation of a 120 mm gel as a function of solenoid current for gels containing (a) 2.45 and (b) 4.9 wt% magnetite.

Upon applying a current to the solenoid, the downward force and the elongation of the material can be measured. Fig. 10(B) shows typical curves for the dependence of the elongation of *ca.* 120 mm long gels. Upon applying current to the solenoid, up to a 10% deformation can be achieved. Other magnetic field geometries produce different deformation effects.

Since the swelling and shrinking behavior of hydrogels is extremely sensitive to many environmental factors, it may conceivably be used as a sensing event if a suitable transduction method can be found. Nanoparticles have been shown to provide methodologies for transducing these changes. By one method, crystalline colloid arrays (CCAs) of polystyrene particles (*ca.* 100 nm diameter) inside hydrogel matrices were constructed.[65] The assembly acts as a diffraction grating with a periodicity dependent on the interparticle spacing. It was found that the swelling and shrinking of the gel, brought about by exposure to different solutes or temperatures (depending on the nature of the gel used), causes the entire assembly to deform, thus increasing or decreasing the unit cell size of the crystallized colloid array. This change is easily detected and quantified by examination of the diffraction properties of the assembly. Fig. 11 shows absorbance spectra of a CCA immobilized in a crown ether-containing hydrogel, (**16**). Exposure of the system to Pb^{2+} causes the swelling of the gel as the metal ions are bound to the crown ether. The diffraction properties of the structure follow Bragg's law, and a 0.5% volume change causes a *ca.* 1 nm movement of the diffraction wavelength.

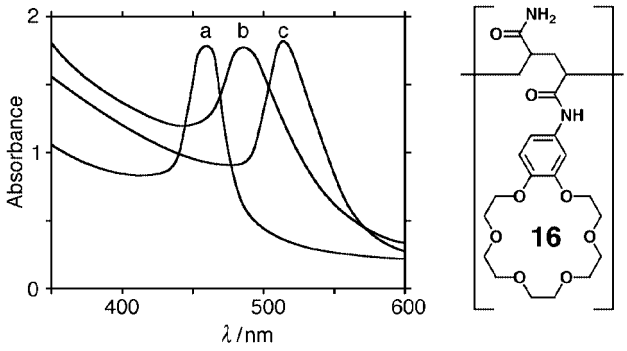

Fig. 11 Absorbance spectra of a polystyrene CCA embedded (7 wt%) in the polymer **16** (*ca.* 1 crown ether unit per 20 monomer units) in the presence of Pb^{2+} at concentrations of (a) 0, (b) 0.4 and (c) 4 ppm. Pb^{2+} can be sensed with a sensitivity limit of *ca.* 20 ppb.

Poly(acrylamide) hydrogels adopt swollen structures in water, but undergo phase transitions to collapsed states upon exposure to less polar solvents such as acetone. Taking advantage of this phenomenon, hydrogels containing a controllable concentration of gold nanoparticles have been synthesized by the route described in Scheme 3.[66] In this procedure, the nanoparticle-free gel is first synthesized on a conductive support by electropolymerization. The nanoparticles are then introduced into the structure by a 'breathing' method. First, the gel is shrunken by immersing it in acetone. This step removes most of the solvent from the gel. The shrunken gel is then immersed in an aqueous nanoparticle solution. The water causes the gel to swell and take the solution into its structure. As it does so, nanoparticles are introduced, where they become stuck by entanglement and the hydrogen bonding network (the gold nanoparticles bear a citrate surface, so have a high hydrogen bonding potential). This 'breathing' mechanism may be repeated several times to gradually increase the nanoparticle content of the gel, and as more nanoparticles are included, the properties of the gel are modified. The electronic properties of the hydrogel are altered upon the incorporation of the Au-nanoparticles. Fig. 12(A) shows Faradaic impedance spectra (in the form of Nyquist plots) of the hydrogel after three 'breathing' cycles. The diameters of the semicircular regions in the plots are indicative of the interfacial electron transfer resistances between the electrode and a solution-solubilized redox probe.[67] As the amount of Au-nanoparticles increases in the hydrogel, the interfacial electron transfer resistance decreases, implying enhanced conductivity of the hydrogel matrix. The electronic properties of the Au-nanoparticle–hydrogel composite are strongly affected upon phase-transition of the polymer matrix. Fig. 12(B) shows chronopotentiometric transients of the polymer matrix in the swollen [curve (a)] and shrunken [curve (b)] states. For comparison, the chronopotentiometric transients of the Au–polymer composite in the swollen [curve (c)] and shrunken [curve (d)] configurations are given. These chronopotentiometric transients indicate the overpotentials required

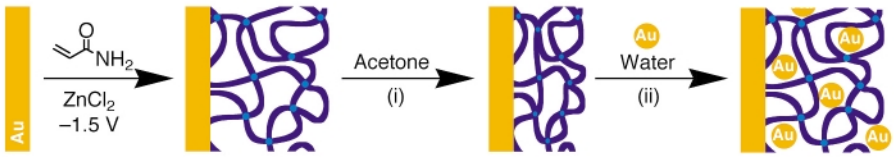

Scheme 3 Method for the assembly of Au-nanoparticle-containing electropolymerized hydrogels by the 'breathing' technique. First the hydrogel is electropolymerized, then the nanoparticles are introduced by (i) shrinking the gel in acetone and (ii) re-swelling the gel in a nanoparticle-containing solution. Steps (i) and (ii) may be repeated to increase the nanoparticle concentration in the gel.

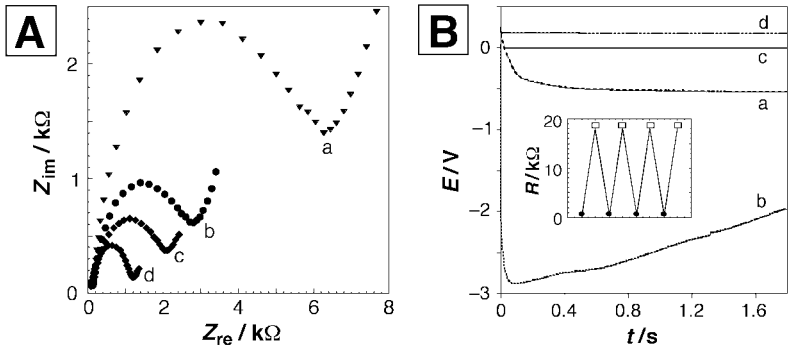

Fig. 12 (A) Faradaic impedance spectra showing the build-up of Au nanoparticles inside a polyacrylamide electrode and the decrease of the interfacial electron transfer resistance: (a) The swollen polyacrylamide gel prior to the introduction of Au-nanoparticles. (b)–(d) The swollen polyacrylamide gel after one, two and three 'breathing' cycles that introduce Au-nanoparticles into the polymer. (B) Chronopotentiometry transients of: (a) the swollen polyacrylamide electrode; (b) the shrunken polyacrylamide gel-electrode; (c) the swollen Au-nanoparticle-containing polyacrylamide electrode; (d) the shrunken Au-nanoparticle-containing polyacrylamide electrode. Inset: reversible switching of the nanoparticle-containing polyacrylamide electrode between swollen (□) and shrunken (●) states.

to retain a constant current in the cell in the presence of a redox label [$Fe(CN)_6^{3-/4-}$], and thus allows the extraction of the values of electrode resistance in the different configurations. The shrunken nanoparticle-free electrode reveals a substantially higher resistance than the swollen configuration (> 300 *vs.* 70 kΩ). On the other hand the shrunken nanoparticle-containing electrode reveals a substantially lower resistance than its swollen state (0.4 *vs.* 20 kΩ, respectively). The low resistance of the shrunken Au-nanoparticle polymer composite is attributed to electrical contact in the nanoparticle network which offers a route for electronic communication between the electrode and the electrolyte solution.

Conclusions and perspectives

The article has addressed means to tailor functional metal and semiconductor nanoparticle arrays for sensoric and electronic uses. The unique conductivity, catalytic, photonic, optical, electronic and photoelectronic properties of metallic and semiconductor nanoparticle systems, originating from the collective interactions in the crosslinked architectures, introduce new perspectives in nanotechnology. The nanostructuring of the assemblies provide high surface-area systems of controllable electronic and optical properties. Crosslinking of nanoparticles with molecular receptors yields conductive arrays with specific recognition features and controllable porosity, and the integration of nanoparticles with polymeric hydrogels paves the way to design signal-triggered materials with novel electronic properties. The conjugation of nanoparticles with nucleic acids establishes a fascinating research area that enables the amplified optical electronic and photoelectrochemical detection of DNA as well as the nanoengineering of predesigned and programmed DNA/nanoparticle circuitry. The application of these methodologies for gene analyses on DNA arrays, and the organization of wired nanoparticle assemblies that include resistance, capacitance and conductivity elements seem to be reachable goals.

We have already discussed some basic nanoparticle-based devices that have found commercial interest such as gas sensors, electrochemical sensors, photovoltaic cells, and luminescence collectors. More advanced applications that use layered nanoparticle composites may need more time to develop, yet they are certainly emerging. For example, nanoparticles may have a large impact in the area of reflective, bistable electronic displays.[68] These displays, known as 'electronic paper', promise to resemble paper in their ease of viewing and portability, without requiring a continuous input of energy to maintain a picture. These technologies are based on variously colored nanoparticles that are aligned inside microcapsules by external electrical fields. Other promising applications of nanoparticles may include displays and memory devices based on electroluminescence matrices[69] or integrated molecule/nanoparticle systems as computing devices.

One important future challenge will involve the organization of addressable nanoparticle architectures of variable composition and functions. Primary efforts in patterning of nanoparticle structures on surfaces have been reported.[70] The rapid advances in developing scanning microscopy 'writing' techniques[71] suggest that the use of 'nanoparticle inks' for nanometer-sized writing is a feasible goal. The progress in the photonic activation of nanometer-sized domains using near-field scanning optical microscopy (NSOM), indicates that the photonic addressability and imaging of nanostructures are viable concepts.

Acknowledgements

Part of the studies are supported by the German–Israel Research Program (DIP). The Max-Planck Award for International Cooperation (I. W.) is acknowledged. A. N. S. gratefully acknowledges a Valazzi Pikovsky fellowship.

Notes and references

1 *Nanosystems, Molecular Machinery, Manufacturing and Computation*, ed. K. E. Drexler, Wiley, New York, 1992; P. Ball, *Nature*, 1993, **362**, 123; P. Ball and L. Garwin, *Nature*, 1992, **355**, 761; *Molecular Electronics*, ed. G. J. Ashwell, Wiley, New York, 1992.
2 A. N. Shipway and I. Willner, *Acc. Chem. Res.*, 2001, **34**, 421; A. N. Shipway, E. Katz and I. Willner, *Struct. Bonding (Berlin)*, 2001, **99**, 237.
3 A. N. Shipway, E. Katz and I. Willner, *Chem. Phys. Chem.*, 2000, **1**, 18.
4 G. Schmid, *Chem. Rev.*, 1992, **92**, 1709; N. Toshima and T. Yonezawa, *New J. Chem.*, 1998, **11**, 1179.
5 H. Weller and A. Eychmüller, *Adv. Photochem.*, 1995, **20**, 165.
6 *Clusters and Colloids*, ed. G. Schmid, VCH, Weinheim, Germany, 1994; P. Mulvaney, *Langmuir*, 1996, **12**, 788; L. E. Brus, *Appl. Phys. A*, 1991, **53**, 465.
7 L. N. Lewis, *Chem. Rev.*, 1993, **93**, 2693; M. Haruta, *Catal. Today*, 1997, **36**, 153.
8 H. Bönnemann and G. A. Braun, *Chem. Eur. J.*, 1997, **3**, 1200.
9 M. M. Maye, Y. Lou and C.-J. Zhong, *Langmuir*, 2000, **16**, 7520.
10 A. C. Templeton, W. P. Wuelfing and R. W. Murray, *Acc. Chem. Res.*, 2000, **33**, 27.
11 A. N. Shipway, M. Lahav and I. Willner, *Adv. Mater.*, 2000, **12**, 993.
12 X. G. Peng, T. E. Wilson, A. P. Alivisatos and P. G. Schultz, *Angew. Chem., Int. Ed. Engl.*, 1997, **36**, 145; L. C. Brousseau, J. P. Novak, S. M. Marikanos and D. L. Feldheim, *Adv. Mater.*, 1999, **11**, 447.
13 A. P. Alivisatos, K. P. Johnsson, X. Peng, T. E. Wilson, C. J. Loweth, M. P. Bruchez Jr. and P. G. Schultz, *Nature*, 1996, **382**, 609.
14 A. N. Shipway, M. Lahav, R. Gabai and I. Willner, *Langmuir*, 2000, **16**, 8789; M. D. Musick, D. J. Peña, S. L. Botsko, T. M. McEvoy, J. N. Richardson and M. J. Natan, *Langmuir*, 1999, **15**, 844.
15 C. Demaille, M. Brust, M. Tsionsky and A. J. Bard, *Anal. Chem.*, 1997, **69**, 2323; A. K. Boal, F. Ilhan, J. E. Derouchey, T. Thurn-Albrecht, T. P.

Russell and V. M. Rotello, *Nature*, 2000, **404**, 746; O. D. Velev, A. M. Lenhoff and E. W. Kaler, *Science*, 2000, **287**, 2240.
16 G. Hornyak, M. Kröll, R. Pugin, T. Sawitowski, G. Schmid, J.-O. Bovin, G. Karsson, H. Hofmeister and S. Hopfe, *Chem. Eur. J*., 1997, **3**, 1951; M. Sano, A. Kamino and S. Shinkai, *Langmuir*, 1999, **15**, 13; S.-W. Chung, G. Markovich and J. R. Heath, *J. Phys. Chem. B*, 1998, **102**, 6685; M. Li, H. Schnablegger and S. Mann, *Nature*, 1999, **402**, 393.
17 C. J. Kiely, J. Fink, J. G. Zheng, M. Brust, D. Bethell and D. J. Schiffrin, *Adv. Mater*., 2000, **12**, 640; L. Motte, F. Billoudet, E. Lacaze, J. Douin and M. P. Pileni, *J. Phys. Chem. B*, 1997, **101**, 138; M. T. Reetz, M. Winter and B. Tesch, *Chem. Commun*., 1997, 147; T. Sato, D. Brown and B. F. G. Johnson, *Chem. Commun*., 1997, 1007; C. B. Murray, C. R. Kagan and M. G. Bawendi, *Science*, 1995, **270**, 1335; G. Schmid, M. Bäumle and N. Beyer, *Angew. Chem., Int. Ed*., 2000, **39**, 181; P. V. Braun, P. Osenar and S. I. Stupp, *Nature*, 1996, **380**, 325; W. Shenton, D. Pum and U. B. Sleytr, *Nature*, 1997, **389**, 585.
18 J. Schmitt, G. Decher, W. J. Dressick, S. L. Brandow, R. E. Geer, R. Shashidhar and J. M. Calvert, *Adv. Mater*., 1997, **9**, 61; D. L. Feldheim, K. C. Grabar, M. J. Natan and T. E. Mallouk, *J. Am. Chem. Soc*., 1996, **118**, 7640; R. Iler, *J. Colloid. Interface Sci*., 1996, **21**, 569.
19 D. I. Gittins, D. Bethell, D. J. Schiffrin and R. J. Nichols, *Nature*, 2000, **408**, 67.
20 S. J. Green, J. J. Stokes, M. J. Hostetler, J. Pietron and R. W. Murray, *J. Phys. Chem. B*, 1997, **101**, 2663; B. Sweryda-Krawiec, T. Cassagneau and J. H. Fendler, *Adv. Mater*., 1999, **11**, 659; R. P. Andres, T. Bein, M. Dorogi, S. Feng, J. I. Henderson, C. P. Kubiak, W. Mahoney, R. G. Osifchin and R. Reifenberger, *Science*, 1996, **272**, 1323; T. Sato, H. Ahmed, D. Brown and B. F. G. Johnson, *J. Appl. Phys*., 1997, **82**, 696; T. Sato and H. Ahmed, *Appl. Phys. Lett*., 1997, **70**, 2759.
21 J. Zhao, R. W. Henkens, J. Stonehuerner, J. P. O'Daly and A. L. Crumbliss, *J. Electroanal. Chem*., 1992, **327**, 109; S. Yabuki and F. Mitzutani, *Electroanalysis*, 1997, **9**, 23.
22 K. R. Brown, A. P. Fox and M. J. Natan, *J. Am. Chem. Soc*., 1996, **118**, 1154.
23 H. Wohltjen and A. W. Snow, *Anal. Chem*., 1998, **70**, 2856.
24 B. L. Doleman, M. C. Lonergan, E. J. Severin, T. P. Vaid and N. S. Lewis, *Anal. Chem*., 1998, **70**, 4177; M. C. Lonergan, E. J. Severin, B. J. Doleman, S. A. Beaber, R. H. Grubbs and N. S. Lewis, *Chem. Mater*., 1996, **8**, 2298; E. J. Severin, B. J. Doleman and N. S. Lewis, *Anal. Chem*., 2000, **72**, 658.
25 A. Doron, E. Katz and I. Willner, *Langmuir*, 1995, **11**, 1313; R. G. Freeman, K. C. Grabar, K. J. Allison, R. M. Bright, J. A. Davis, A. P. Guthrie, M. B. Hommer, M. A. Jackson, P. C. Smith, D. G. Walter and M. J. Natan, *Science*, 1995, **267**, 1629; G. Chumanov, K. Sokolov, B. W. Gregory and T. M. Cotton, *J. Phys. Chem*., 1995, **99**, 9466.
26 A. N. Shipway, M. Lahav, R. Blonder and I. Willner, *Chem. Mater*., 1999, **11**, 13.
27 M. Lahav, A. N. Shipway, I. Willner, M. B. Nielsen and J. Fraser Stoddart, *J. Electroanal. Chem*., 2000, **482**, 217.
28 M. Lahav, R. Gabai, A. N. Shipway and I. Willner, *Chem. Commun*., 1999, 1937.
29 M. Miyake, H. Matsumoto, M. Nishizawa, T. Sakata, H. Mori, S. Kuwabata and H. Yoneyama, *Langmuir*, 1997, **13**, 742; K. Ariga, Y. Lvov, M. Onda, I. Ichinose and T. Kunitake, *Chem. Lett*., 1997, 125; D. L. Feldheim, K. C. Grabar, M. J. Natan and T. E. Mallouk, *J. Am. Chem. Soc*., 1996, **118**, 7640.
30 E. Hao, B. Yang, J. Zhang, X. Zhang, J. Sun and J. Shen, *J. Mater. Chem*., 1998, 1327; R. Iler, *J. Colloid. Interface Sci*., 1996, **21**, 569; A. Kumar, A. B. Mandale and M. Sastry, *Langmuir*, 2000, **16**, 6921.
31 F. Patolsky, T. Gabriel and I. Willner, *J. Electroanal Chem*., 1999, **479**, 69.
32 M. Brust, R. Etchenique, E. J. Calvo and G. J. Gordillo, *Chem. Commun*., 1996, 1949; M. D. Musick, C. D. Keating, M. H. Keefe and M. J. Natan, *Chem. Mater*., 1997, **9**, 1499.
33 S. Norman, T. Andersson, C. G. Granqvist and O. Hunderi, *Phys. Rev. B*, 1978, **18**, 674; R. H. Dormeus, *J. Appl. Phys*., 1996, **37**, 2775.
34 M. Quinten and U. Kreibig, *Surf. Sci*., 1986, **172**, 557; K. C. Grabar, K. J. Allison, B. E. Baker, R. M. Bright, K. R. Brown, R. G. Freeman, A. P. Fox, C. D. Keating, M. D. Musick and M. J. Natan, *Langmuir*, 1996, **12**, 2353.
35 B. Odell, M. V. Reddington, A. M. Z. Slawin, N. Spencer, J. F. Stoddart and D. J. Williams, *Angew. Chem., Int. Ed. Engl*., 1998, **27**, 1547.
36 M. Lahav, A. N. Shipway and I. Willner, *J. Chem. Soc., Perkin Trans. 2*, 1999, 1925.
37 M. Asakawa, P. R. Ashton, S. Menzer, F. M. Raymo, J. F. Stoddart, A. J. P. White and D. J. Williams, *Chem. Eur. J*., 1996, **2**, 877.
38 M. Fujita, J. Yazaki and K. Ogara, *Tetrahedron Lett*., 1991, **32**, 5589.
39 A. B. Kharitonov, A. N. Shipway and I. Willner, *Anal. Chem*., 1999, **71**, 5441.
40 Y. Z. Hu, S. H. Bossmann, D. van Loyen, O. Schwarz and H. Dürr, *Chem. Eur. J*., 1999, **5**, 1267.
41 M. Lahav, V. Heleg-Shabtai, J. Wasserman, E. Katz, I. Willner, H. Dürr, Y.-Z. Hu and S. H. Bossmann, *J. Am. Chem. Soc*., 2000, **122**, 11 480.
42 M. Lahav, T. Gabriel, A. N. Shipway and I. Willner, *J. Am. Chem. Soc*., 1999, **121**, 258.
43 M. Grätzel, Nanocrystalline Electronic Junctions, in *Semiconductor Nanoclusters—Physical, Chemical and Catalytic Aspects*, ed. P. V. Kamat and D. Meisel, Elsevier, Amsterdam, 1997, p. 353; P. V. Kamat, Electron-Transfer Processes in Nanostructured Semiconductor Thin Films, in *Nanoparticles and Nanostructural Films*, ed. J. Fendler, Wiley-VCH, New York, 1998, p. 207.
44 B. O'Regan and M. Grätzel, *Nature*, 1991, **353**, 737; U. Bach, D. Lupo, P. Comte, J. E. Moser, F. Weissortel, J. Salbeck, H. Spreitzer and M. Grätzel, *Nature*, 1998, **395**, 583; S. D. Burnside, V. Shklover, C. Barbé, P. Comte, F. Arendse, K. Brooks and M. Grätzel, *Chem. Mater*., 1998, **10**, 2419; D. Matthews, A. Kay and M. Grätzel, *Aust. J. Chem*., 1994, **47**, 1869; L. Kavan, M. Grätzel, J. Rathousky and A. Zukal, *J. Electrochem. Soc*., 1996, **143**, 394; V. Shklover, M.-K. Nazeeruddin, S. M. Zakeeruddin, C. Barbé, A. Kay, T. Haibach, W. Steurer, R. Hermann, H.-U. Nissen and M. Grätzel, *Chem. Mater*., 1997, **9**, 430.
45 T. Cassagneau, T. E. Mallouk and J. H. Fendler, *J. Am. Chem. Soc*., 1998, **120**, 7848; V. L. Colvin, M. C. Schlamp and A. P. Alivisatos, *Nature*, 1994, **370**, 354; N. D. Kumar, M. P. Joshi, C. S. Friend, P. N. Prasad and R. Burzynski, *Appl. Phys. Lett*., 1997, **71**, 1388; M. Gao, B. Richter and S. Kirstein, *Adv. Mater*., 1997, **9**, 802; S. A. Carter, J. C. Scott and P. J. Brock, *Appl. Phys. Lett*., 1997, **71**, 1145.
46 L. Spanhel, H. Weller and A. Henglein, *J. Am. Chem. Soc*., 1987, **109**, 6632; K. R. Godipas, M. Bohorquez and P. V. Kamat, *J. Phys. Chem*., 1990, **94**, 6435; N. Serpone, E. Borgarello and M. Grätzel, *J. Chem. Soc., Chem. Commun*., 1984, 342; P. Pichat, E. Borgarello, J. Disdier, J.-M. Herrmann, E. Pelizzetti and N. Serpone, *J. Chem. Soc., Faraday Trans. 1*, 1988, **84**, 261; N. Serpone, E. Borgarello and E. Pelizzetti, *J. Electrochem. Soc*., 1988, **135**, 2760; D. Lawless, S. Kapoor and D. Meisel, *J. Phys. Chem. B*, 1995, **99**, 10329.
47 K. Barnham, J. L. Marques and J. Hassard, *Appl. Phys. Lett*., 2000, **76**, 1197.
48 W. H. Weber and J. Lambe, *Appl. Opt*., 1976, **15**, 2299; A. Goetzberger and W. Greubel, *Appl. Phys*, 1977, **14**, 123.
49 O. I. Micic, K. M. Jones, A. Cahill and A. J. Nozic, *J. Phys. Chem. B*, 1998, **102**, 9791.
50 C. R. Kagan, C. B. Murray and M. G. Bawendi, *Phys. Rev. B*, 1999, **54**, 8633.
51 C. Nasr, P. V. Kamat and S. Hotchandani, *J. Electroanal. Chem*., 1997, **420**, 201.
52 S. Hotchandani and P. V. Kamat, *J. Phys. Chem*., 1992, **96**, 6834.
53 R. Vogel, K. Pohl and H. Weller, *Chem. Phys. Lett*., 1990, **174**, 241; S. Hotchandani and P. V. Kamat, *Chem. Phys. Lett*., 1992, **191**, 320.
54 A. Zaban, S. G. Chen, S. Chappel and B. A. Gregg, *Chem. Commun*., 2000, 2231.
55 C. Nasr, S. Hotchandani, W. Y. Kim, R. S. Schmehl and P. V. Kamat, *J. Phys. Chem. B*, 1997, **101**, 7480.
56 N. C. Seeman, *Acc. Chem. Res*., 1997, **30**, 357; C. M. Niemeyer, *Angew. Chem., Int. Ed. Engl*., 1997, **36**, 585.
57 E. Braun, Y. Eichen, U. Sivan and G. Ben-Yoseph, *Nature*, 1998, **391**, 775.
58 R. Elghanian, J. J. Storhoff, R. C. Mucic, R. L. Letsinger and C. A. Mirkin, *Science*, 1997, **277**, 1078; J. J. Storhoff, R. Elghanian, R. C. Mucic, C. A. Mirkin and R. L. Letsinger, *J. Am. Chem. Soc*., 1998, **120**, 1959; C. A. Mirkin, R. L. Letsinger, R. C. Mucic and J. J. Storhoff, *Nature*, 1996, **382**, 607.
59 (*a*) F. Patolsky, K. T. Ranjit, A. Lichtenstein and I. Willner, *Chem. Commun*., 2000, 1025; (*b*) A. T. Taton, R. C. Mucic, C. A. Mirkin and R. L. Letsinger, *J. Am. Chem. Soc*., 2000, **122**, 6305.
60 I. Willner, F. Patolsky and J. Wasserman, *Angew. Chem., Int. Ed*., 2001, **105**, 4205.
61 D. Y. Godovsky, *Adv. Polym. Sci*., 2000, **153**, 163.
62 T. Tanaka, I. Nishio, S.-T. Sun and S. Uneo-Nishio, *Science*, 1982, **218**, 467; T. Oya, T. Enoki, A. Y. Grosberg, S. Masamune, T. Sakiyama, Y. Takeoka, K. Tanaka, G. Wang, Y. Yilmaz, M. S. Feld, R. Dasari and T. Tanaka, *Science*, 1999, **286**, 1543; T. G. Park and A. S. Hoffman, *J. Appl. Polym. Sci*., 1992, **46**, 659; J. H. Holtz, J. S. W. Holtz, C. H. Munro and S. A. Asher, *Anal. Chem*., 1998, **70**, 780.
63 M. Zrínyi, L. Barsi and A. Büki, *J. Chem. Phys*., 1996, **104**, 8750; M. Zrínyi, L. Barsi, D. Szabó and H.-G. Kilian, *J. Chem. Phys*., 1997, **106**, 5685.
64 C. R. Mayer, V. Cabuil, T. Lalot and R. Thouvenot, *Angew. Chem., Int. Ed*., 1999, **38**, 3672.
65 J. M. Weissman, H. B. Sunkara, A. S. Tse and S. A. Asher, *Science*, 1996, **274**, 959; J. H. Holtz and S. A. Asher, *Nature*, 1997, **389**, 829.
66 V. Pardo-Yissar, R. Gabai, T. Bourenko, A. N. Shipway and I. Willner, *Adv. Mater*., 2001, **13**, 1320.

67 A. J. Bard and L. R. Faulkner, *Electrochemical Methods: Fundamentals and Applications*, Wiley, New York, 1980.
68 B. Comiskey, J. D. Albert, H. Yoshizawa and J. Jacobson, *Nature*, 1998, **394**, 253; R. Dagani, *Chem. Eng. News*, 2001, Jan 15, 40.
69 V. L. Colvin, M. C. Schlamp and A. P. Alivisatos, *Nature*, 1994, **370**, 354; B. O. Dabbousi, M. G. Bawendi, O. Onitsuka and M. F. Rubner, *Appl. Phys. Lett*., 1995, **66**, 1316.
70 J. Liu, L. Zhang, P. Mao, D. Chen, N. Gu, J. Ren, Y. Wu and Z. Lu, *Chem. Lett*., 1997, 1147; J.-F. Liu, L.-G. Zhang, J.-Y. Ren, Y.-P. Wu, Z.-H. Lu, P.-S. Mao and D.-Y. Chen, *Thin Solid Films*, 1998, **327**–**329**, 176; T. Vossmeyer, E. DeIonno and J. R. Heath, *Angew. Chem., Int. Ed. Engl*., 1997, **36**, 1080; W. J. Dressick, C. S. Dulcey, S. L. Brandow, H. Witschi and P. F. Neeley, *J. Vac. Sci. Technol. A*, 1999, **17**, 1432; S. L. Brandow, M.-S. Chen, R. Aggarwal, C. S. Dulcey, J. M. Calvert and W. J. Dressick, *Langmuir*, 1999, **15**, 5429; P. C. Hidber, W. Helbig, E. Kim and G. M. Whitesides, *Langmuir*, 1996, **12**, 1375; J. L. Coffer, S. R. Bigham, R. F. Pinizzotto and H. Yang, *Nanotechnology*, 1992, **3**, 69.
71 F. P. Zamborini and R. M. Crooks, *J. Am. Chem. Soc*., 1998, **120**, 9700; R. D. Piner, J. Zhu, F. Xu, S. H. Hong and C. A. Mirkin, *Science*, 1999, **283**, 661; R. Resch, C. Baur, A. Bugacov, B. E. Koel, A. Madhukar, A. A. G. Requicha and P. Will, *Langmuir*, 1998, **14**, 6613; S. L. Brandow, W. J. Dressick, C. S. Dulcey, T. S. Koloski, L. M. Shirey, J. Schmidt and J. M. Calvert, *J. Vac. Sci. Technol. B*, 1997, **15**, 1818; A. Doron, E. Joselevich, A. Schlittner and I. Willner, *Thin Solid Films*, 1999, **340**, 183; M. T. Reetz and M. Winter, *J. Am. Chem. Soc*., 1997, **119**, 4539.